

Unveiling the Intricacies of Acute Aortic Syndromes through Imaging: A Case Series

MADHU SHANKAR KIKKERI¹, R VIDHYA RANI², D NAVEEN³, MR AKSHAY⁴, S LEELASHREE⁵

CC BY-NC-ND

ABSTRACT

Acute Aortic Syndrome (AAS) comprises of three distinct pathological conditions: Aortic Dissection (AD), Penetrating Atherosclerotic Ulcer (PAU), and Intramural Haematoma (IMH). Although AAS and its emergencies are not common occurrences, they are considered highly dangerous and potentially fatal. Clinically, differentiating between the various types of aortic syndromes can be challenging. The prognosis of these conditions significantly depends on speedy and precise analysis. Therefore, present study emphasised the critical role of radiology in the diagnosis of AASs, with Contrast-Enhanced Computed Tomography (CECT) being the quickest and most consistent imaging modality. In this case series, four cases of AASs are presented, comprising three cases of AD and a case of PAU in a patient with infrarenal aortic occlusion. Notably, one of the dissection cases was accompanied by renal ischaemia. Recognising acute aortic emergencies promptly is essential for saving lives.

Keywords: Aortic dissection, Penetrating atherosclerotic ulcer, Intramural haematoma

INTRODUCTION

The AAS encompasses three pathological conditions: PAU, AD, and IMH [1]. Although relatively rare in the general population, occurring at a rate of 3.5 to 6.0 cases per 100,000 patients per year, AAS carries a high mortality rate [2]. Aortic trauma accounts for 80-90% of fatalities, with type A AD contributing to mortality rates of 50-60% [2,3]. Given that acute AD is the most prevalent condition among AASs, accurate recognition and classification of AD is a crucial and potentially life-saving endeavour [3,4].

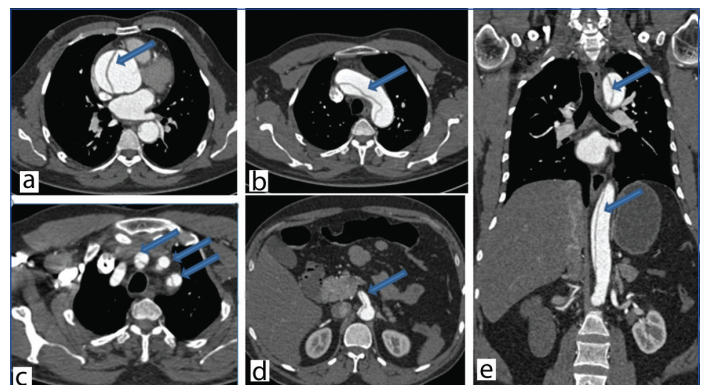
CASE SERIES

Case 1

A 33-year-old male patient, hypertensive for three years with a history of non compliance to medications, presented with severe chest and epigastric pain for one day. His Blood Pressure (BP) at admission was 180/120 mmHg. Bedside 2D Echocardiography (2D ECHO) revealed a dissection flap in the ascending aorta. He was referred for an emergency CT aortogram, which revealed a long segment dissection flap in the aortic root, ascending aorta, aortic arch, descending thoracic aorta, and abdominal aorta extending to the level of the infrarenal abdominal aorta [Table/Fig-1a,b-e]. The dissection flap was further seen extending into the proximal portion of the aortic arch branches [Table/Fig-1c] and the superior mesenteric artery [Table/Fig-1d]. The maximum aortic dimension was measured to be 5.1cm. The celiac trunk and left renal artery were seen arising from the False Lumen (FL), and the right renal artery from the True Lumen (TL) (not shown here). There were no features of any solid organ/bowel ischaemia. Based on imaging findings, a diagnosis of Stanford Type A AD was made [5]. Surgical treatment was proposed to the patient, but it was declined by the caregivers. He was discharged against medical advice and subsequently lost to follow-up.

Case 2

A 65-year-old male diabetic patient with complaints of increased frequency and burning during urination for the past five days was sent for a sonographic assessment to rule out cystitis. There was no relevant past or family history. The ultrasound of the abdomen and pelvis showed an incidental finding of ectatic dilation of the proximal

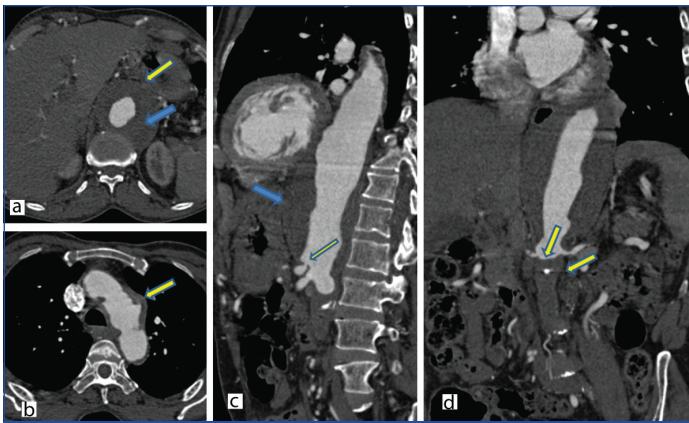


[Table/Fig-1]: Aortic Dissection (AD): (a,b) Axial sections of the upper thorax in arterial phase showing intimal flap in the ascending aorta and aortic arch (blue arrows) dividing it into a false and true lumen (TL); (c) Axial sections at the level of aortic arch branches showing dissection flap extending into the proximal portion of the brachiocephalic trunk, left common carotid and left subclavian arteries (blue arrows); (d) Axial section in arterial phase at the level of superior mesenteric artery origin showing extension of the dissection flap into the superior mesenteric artery (blue arrow), and (e) Coronal CT image in arterial phase showing a long segment dissection flap involving the descending thoracic and proximal abdominal aorta (blue arrows)

abdominal aorta with a peripheral thrombus. A CT aortogram was performed, which showed fusiform aneurysmal dilatation of the distal descending thoracic aorta and upper abdominal aorta with concentric peripheral mural thrombus [Table/Fig-2a,c,d]. Diffuse irregular atherosclerotic wall thickening was noted in the arch with focal outpouching of contrast on its lateral aspect, representing a PAU [Table/Fig-2b]. There was complete luminal occlusion of the infrarenal portion of the abdominal aorta till the bilateral proximal common iliac arteries [Table/Fig-2d], with good distal reformation (not shown here). As there was good distal run-off, the patient was conservatively managed for pain relief and hypertension. However, he was lost to further follow-up.

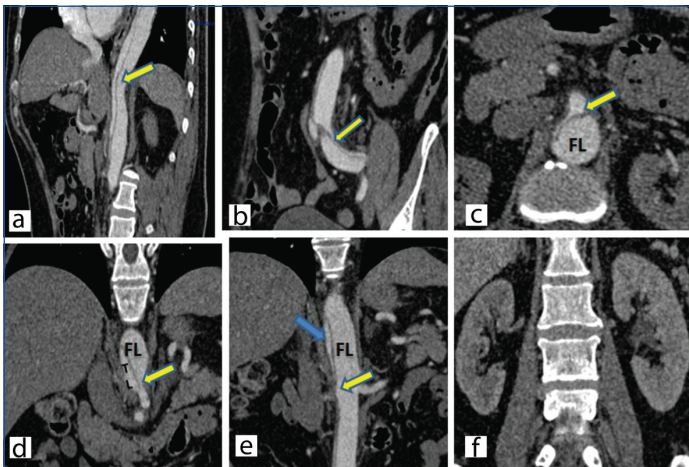
Case 3

A 44-year-old male presented to the hospital with complaints of bilateral lower limb pitting oedema for one week. Upon admission, his blood pressure was 270/140 mmHg. Fundus examination revealed grade III papilloedema. There was no contributory past or family history. Laboratory investigations revealed raised urea and



[Table/Fig-2]: (a) Axial CT section in arterial phase showing dilated proximal abdominal aorta (yellow arrow) with circumferential mural thrombus (blue arrow); (b) Axial CT section at the aortic arch level showing diffuse atherosclerotic wall thickening with focal outpouching of contrast (yellow arrow) on its lateral aspect representing a PAAU; (c) Sagittal CT section in arterial phase showing aneurysmal dilatation of distal descending thoracic aorta and proximal abdominal aorta with concentric mural thrombus (blue arrow); (d) Coronal reformatted CT image in the arterial phase showing complete non opacification of the infrarenal abdominal aorta (yellow arrows) representing infrarenal aortic occlusion.

creatinine levels of 70 mg/dL and 3.5 mg/dL, respectively, at the time of admission. A 2D ECHO revealed concentric left ventricular hypertrophy with Grade III left ventricular diastolic dysfunction. Despite treatment with 3-4 antihypertensives (intravenous infusion of labetalol at 120mg/hour, nitroglycerin infusion at 20 µg/minute, tablet nicardia XL 30 mg TID, tablet metoprolol 50 mg BD, tablet minipress XL 5mg BD), his blood pressure remained uncontrolled. To investigate potential secondary causes of hypertension, a renal artery Doppler was performed, revealing tardus parvus waveforms in the segmental renal arteries on the right-side. A CT renal angiogram was performed, revealing a long segment intimal flap in the visualised part of the distal descending thoracic aorta, abdominal aorta, and left common iliac artery with a very small TL in the juxtarenal and infrarenal portions [Table/Fig-3a,b]. The entry tear could not be assessed as the entire aorta was not imaged. The coeliac artery was observed arising from the small TL [Table/Fig-3c]. The superior mesenteric artery was supplied by both the true and FL [Table/Fig-3d]. The right renal artery was found to be originating from the very small TL with ostioproximal non opacification suggesting thrombosis [Table/Fig-3e]. The right kidney showed decreased contrast enhancement compared to the left [Table/Fig-3f]. The

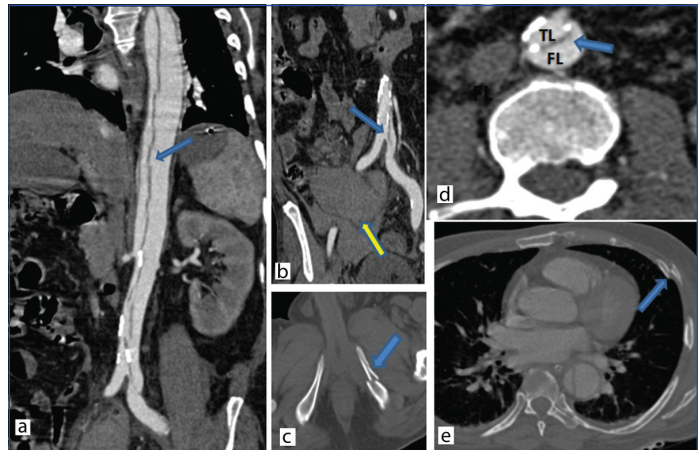


[Table/Fig-3]: Aortic Dissection (AD): (a) Oblique reformatted CT images in arterial phase showing a dissection flap in descending thoracic, abdominal aorta (yellow arrow); (b) Dissection flap is seen extending into the left common iliac artery (yellow arrow) in coronal reformatted images; (c) Axial CT section in the arterial phase showing celiac trunk originating from the smaller TL (yellow arrow) (FL); (d) Coronal reformatted images at the level of superior mesenteric artery origin showing that it is supplied by both false and TLs; (e) Coronal CT images in the arterial phase showing very small TL (blue arrow) and larger FL. Right renal artery is originating from the TL with non opacification in its ostioproximal segment representing thrombosis (yellow arrow); (f) Coronal CT section in the arterial phase showing relatively hypoenhancing right kidney when compared to the left kidney.

patient underwent dialysis postcontrast study, and the patient's BP at discharge was 180/100 mm Hg with nitroglycerine infusion. He was discharged with advice to strictly adhere to his blood pressure medications and undergo regular CT scans to monitor changes. However, the patient did not return for further follow-up.

Case 4

A 66-year-old male patient, a known case of Parkinson's disease, presented to the hospital with an alleged history of accidental fall from height five hours before arriving at the hospital. On examination, the patient was unconscious with a Glasgow Coma Scale (GCS) of E1M3V1. A CT Brain was performed, which showed haemorrhagic contusions in the bilateral frontal, parietal, left temporal lobes, left capsuloganglionic region, subarachnoid haemorrhage along the right parietal sulcal space, and diffuse cerebral oedema. He was put on antioedema measures and antiepileptics. Due to a drop in haemoglobin, a contrast-enhanced CT of the abdomen and pelvis was advised, which showed a long segment intimal flap extending from the proximal descending thoracic aorta to the aortic bifurcation, further extending into the left common iliac artery resulting in the formation of a true and FL [Table/Fig-4a,b,d]. A mesenteric haematoma was seen in the right iliac fossa [Table/Fig-4b]. The bone window showed fractures in the left inferior pubic ramus, left-sided ribs [Table/Fig-4c,e], the inferior aspect of the left hemisacrum, and the left transverse processes of the L2, L4, and L5 vertebrae (not shown here). Due to pelvic bone fractures and a low GCS, conservative management was pursued. He was then referred to a higher centre for further management.



[Table/Fig-4]: Aortic Dissection (AD): (a) Coronal oblique reformatted CT image in arterial phase showing a long segment intimal flap in descending thoracic and abdominal aorta (blue arrow) dividing it into a smaller true and larger False Lumen (FL). Ascending aorta and aortic arch were normal (not shown here); (b) Coronal oblique reformatted CT image showing the extension of the dissection flap into left common iliac artery (blue arrow). Mesenteric haematoma (yellow arrow) noted in the right iliac fossa region; (c) Axial CT image in bone window showing fracture in the left inferior pubic ramus (blue arrow); (d) Axial CT image in arterial phase showing an intimal flap dividing the lumen into smaller True Lumen (TL) and larger False Lumen (FL). Intimal and wall calcification noted around the TL (blue arrow); (e) Axial CT image in bone window showing fracture in the lateral aspect of the left 6th rib (blue arrow).

DISCUSSION

The AAS includes three distinct pathological conditions- AD, accounting for 85-95% of AAS cases; PAAU, representing 2-7%; and IMH, ranging from 0-25%. There are two different classification systems to differentiate between types of AAS and to guide management. The Stanford classification [5] separates type A, which involves the ascending aorta, from type B, which does not involve the ascending aorta. The De Bakey classification [4] distinguishes type I, which involves at least the ascending aorta and the aortic arch and often also the descending aorta, type II, which is confined to the ascending aorta, and type III, which originates in the descending aorta distal to the left subclavian artery [4,5]. Reliable diagnostic tools such as CT, Magnetic Resonance Imaging (MRI), and Transesophageal Echocardiography (TOE) are commonly used for AAS diagnosis [2]. CT aortogram is an ideal

modality for deciding on surgical or non surgical management in AAS patients. In addition, CT aortogram can detect aortic injuries and ruptured aortic aneurysms even in asymptomatic cases [6].

Aortic Dissection (AD): In AD, high-pressure blood penetrates an intimal tear, causing the layers of the aortic wall to separate and form a FL. Typically, the pressure within this FL is higher and more constant than the TL due to restricted distal blood flow, which leads to dynamic or static compression of the TL. As a result, the TL often becomes smaller or even completely occluded, resulting in malperfusion of aortic side branches and subsequent ischaemia or infarction of end organs. Any aortic side branch can be affected, including the coronary arteries, cervical branches, spinal arteries, visceral arteries, and lower extremity arteries [7]. Accurate CT differentiation between the true and FL has historically been less critical as surgical intervention was the primary treatment approach, with decisions primarily based on the involvement of the ascending aorta. However, with the advancement of percutaneous treatment methods, driven in part by improvements in CT angiography, reliable CT findings distinguishing TL and FL have gained importance. These findings are crucial in aiding cardiovascular surgeons and radiologists in planning endovascular treatment for dissection. It is also crucial to identify the luminal origins of branch vessels before placing endografts or bare stents within the aorta or its branches to ensure optimal deployment and prevent end-organ ischaemia [8].

Penetrating Atherosclerotic Ulcer (PAU): The hallmark of PAU is the loss of tunica intima integrity, usually resulting from erosion of an atherosclerotic plaque. PAU commonly occurs in regions subjected to elevated stress, such as the descending thoracic aorta (90% of the cases) adjacent to the ligamentum arteriosum [1]. The PAU cascade begins with a haematoma and progresses to pseudoaneurysm formation, followed by dissection or rupture. Under the pressure of the underlying haematoma, PAU dissects the aortic intima and media, resulting in the creation of a pseudoaneurysm [9]. The surrounding aortic segment is usually thickened with some degree of enhancement. Inflammatory aneurysm closely resembles PAU and is differentiated from PAU by marked wall thickening and associated fibrosis forming surrounding adhesions [9]. Detecting PAU requires a high clinical suspicion index. PAU limited to the media often presents asymptotically, leading to frequent incidental findings [1], as was in case number 2.

Intramural Haematoma (IMH): Prolonged hypertension triggers a series of histologic changes in the aortic wall, including constriction and occlusion of the vasa vasorum, hypertrophy and hyperplasia of the smooth muscle, and an ischaemic and rigid outer media. The aortic lumen continues to distribute nutrients to the inner media, which maintains its typical flexibility. Increased shear stress at the interface between the inner and outer media, resulting from this elasticity differential, may result in a medial tear, IMH, or AD [5]. In classic AD, the propagation of blood flow across the primary intimal tear leads to the formation of true and false lumen, creating the characteristic “double-channeled aorta” appearance. However, in IMH, there is no intimal tear, and the haemorrhage is contained within the aortic wall. On CT scans, the presence of continuous, typically crescent-shaped areas of high density along the aortic wall before contrast injection, which remain unenhanced after contrast administration, indicates a characteristic finding of IMH. Similarly, MRI can easily identify crescentic thickening of the aortic wall without an intimal flap or tear, with variable signal intensity depending on the level of methaemoglobin within the haematoma. TOE is valuable for visualising circumferential or crescentic thickening of the aortic wall without an intimal tear, revealing the displacement of intimal calcification due to blood accumulation within the aortic media, aiding in differential diagnosis [10]. Mortality

rates are high in cases where IMH progresses to AD. Therefore, the primary objective of IMH therapy is typically to prevent the development of AD or aortic rupture [1].

Chest radiography is the early imaging strategy for acute trauma or chest pain, but contrast-enhanced Computed Tomography Angiography (CTA) is favoured in clinically doubtful cases. CTA efficiently triages aortic emergencies, guiding surgical or non surgical approaches due to its rapidity, non invasiveness, and superior imaging quality [3]. Transesophageal Echocardiography (TEE) and abdominal ultrasound serve as bedside tools for unstable patients but have limitations. Abdominal ultrasound may detect aortic conditions in lean patients, but it is not preferred for diagnosis or follow-up. Magnetic Resonance Angiography (MRA) is an alternative to CTA, especially in cases that require avoiding ionising radiation or iodinated contrast. Non contrast MRA is suitable for patients with renal dysfunction. CTA remains the primary choice, while MRA serves as the common alternative, each with distinct strengths and weaknesses [3]. Current data indicate that open surgical repair is the preferred approach for addressing type A AAS (involving the ascending aorta), while thoracic endovascular aortic repair may be more suitable for type B AAS (affecting the descending aorta) [2].

In the present case series, the three AD cases showed the classical spiral intimal flap with TL and FL formation. This was similar to the findings reported by Duran ES et al., [11]. In one of the cases, AD was seen in a trauma setting. AD can occur spontaneously or secondary to blunt trauma. In present case, AD was diagnosed in the setting of blunt abdominal trauma, but a causal relationship cannot be proven, and the temporal relationship may be coincidentally similar to the case reported by Penn JL et al., [12]. PAU was incidentally detected in a patient with complete infrarenal aortic occlusion and a peripherally thrombosed aortic aneurysm. It was seen as a focal contrast outpouching in the background of diffuse atherosclerotic wall thickening, similar to the case reported by Nathan DP et al., [13].

CONCLUSION(S)

Early detection of AAS is important in patients with acute chest or back pain and hypertension because it is associated with increased mortality. Radiology plays a pivotal role, with initial imaging typically employing radiographs, followed by contrast-enhanced CTA as the preferred method. CTA offers rapid assessment, detailed anatomical information, and the ability to detect complications and guide treatment strategies. This case series emphasises the importance of imaging in cases of AAS.

REFERENCES

- [1] Morris JH, Mix D, Cameron SJ. Acute aortic syndromes: Update in current medical management. *Curr Treat Options Cardiovasc Med.* 2017;19(4):29.
- [2] Mussa FF, Horton JD, Moridzadeh R, Nicholson J, Trimarchi S, Eagle KA. Acute aortic dissection and intramural hematoma: A systematic review. *JAMA.* 2016;316(7):754-63.
- [3] Baliyan V, Parakh A, Prabhakar AM, Hedgire S. Acute aortic syndromes and aortic emergencies. *Cardiovasc Diagn Ther.* 2018;8(Suppl 1):S82-96.
- [4] De Bakey ME, Henly WS, Cooley DA, Morris GC Jr, Crawford ES, Beall AC Jr. Surgical management of dissecting aneurysms of the aorta. *J Thorac Cardiovasc Surg.* 1965;49(1):130-49.
- [5] Gutschow SE, Walker CM, Martínez-Jiménez S, Rosado-de-Christenson ML, Stowell J, Kunin JR. Emerging concepts in intramural hematoma imaging. *Radiographics.* 2016;36(3):660-74.
- [6] Fox N, Schwartz D, Salazar JH, Haut ER, Dahm P, Black JH, et al. Evaluation and management of blunt traumatic aortic injury: A practice management guideline from the Eastern Association for the Surgery of Trauma. *J Trauma Acute Care Surg.* 2015;78(1):136-46.
- [7] Murillo H, Molvin L, Chin AS, Fleischmann D. Aortic dissection and other acute aortic syndromes: Diagnostic imaging findings from acute to chronic longitudinal progression. *Radiographics.* 2021;41(2):425-46.
- [8] LePage MA, Quint LE, Sonnad SS, Deeb GM, Williams DM. Aortic dissection: CT features that distinguish true lumen from false lumen. *AJR Am J Roentgenol.* 2001;177(1):207-11.

- [9] Dev R, Gitanjali K, Anshuman D. Demystifying penetrating atherosclerotic ulcer of aorta: Unrealised tyrant of senile aortic changes. *J Cardiovasc Thorac Res.* 2021;13(1):01-14.
- [10] Song JK. Diagnosis of aortic intramural haematoma. *Heart.* 2004;90(4):368-71.
- [11] Duran ES, Ahmad F, Elshikh M, Masood I, Duran C. Computed tomography imaging findings of acute aortic pathologies. *Cureus.* 2019;11(8) :e5534.
- [12] Penn JL, Martindale JL, Milne LW, Marill KA. Aortic dissection associated with blunt chest trauma diagnosed by elevated D-dimer. *Int J Surg Case Rep.* 2015;10:76-79.
- [13] Nathan DP, Boonn W, Lai E, Wang GJ, Desai N, Woo EY, et al. Presentation, complications, and natural history of penetrating atherosclerotic ulcer disease. *J Vasc Surg.* 2012;55(1):10-15.

PARTICULARS OF CONTRIBUTORS:

1. Assistant Professor, Department of Radiodiagnosis, Sapthagiri Institute of Medical Sciences and Research Centre, Bengaluru, Karnataka, India.
2. Professor, Department of Radiodiagnosis, Sapthagiri Institute of Medical Sciences and Research Centre, Bengaluru, Karnataka, India.
3. Associate Professor, Department of Radiodiagnosis, Sapthagiri Institute of Medical Sciences and Research Centre, Bengaluru, Karnataka, India.
4. Postgraduate Resident, Department of Radiodiagnosis, Sapthagiri Institute of Medical Sciences and Research Centre, Bengaluru, Karnataka, India.
5. Postgraduate Resident, Department of Radiodiagnosis, Sapthagiri Institute of Medical Sciences and Research Centre, Bengaluru, Karnataka, India.

NAME, ADDRESS, E-MAIL ID OF THE CORRESPONDING AUTHOR:

Dr. D Naveen,
Associate Professor, Department of Radiodiagnosis, Sapthagiri Institute of Medical Sciences and Research Centre, Bengaluru-560090, Karnataka, India.
E-mail: drnavrad@gmail.com

PLAGIARISM CHECKING METHODS: [Jain H et al.]

- Plagiarism X-checker: Apr 09, 2024
- Manual Googling: May 15, 2024
- iThenticate Software: Jun 05, 2024 (10%)

ETYMOLOGY: Author Origin**EMENDATIONS:** 6**AUTHOR DECLARATION:**

- Financial or Other Competing Interests: None
- Was informed consent obtained from the subjects involved in the study? Yes
- For any images presented appropriate consent has been obtained from the subjects. Yes

Date of Submission: **Apr 08, 2024**Date of Peer Review: **May 13, 2024**Date of Acceptance: **Jun 06, 2024**Date of Publishing: **Aug 01, 2024**